

AD-A150 964 DEMONSTRATION OF THE FEASIBILITY OF THE TUNING AND STIMULATION OF NUCLEAR RADIATION(U) TEXAS UNIV AT DALLAS RICHARDSON CENTER FOR QUANTUM ELECTRONIC.

AD-A150 964 DEMONSTRATION OF THE FEASIBILITY OF THE TUNING AND STIMULATION OF NUCLEAR RADIATION(U) TEXAS UNIV AT DALLAS RICHARDSON CENTER FOR QUANTUM ELECTRONIC.

1/1

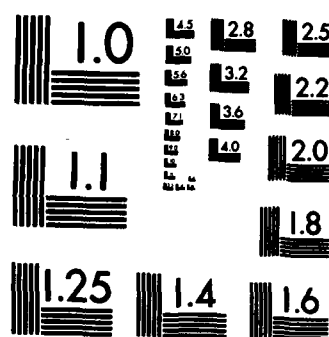
UNCLASSIFIED C B COLLINS 31 JAN 85 N00014-81-K-0653

UNCLASSIFIED C B COLLINS 31 JAN 85 N00014-81-K-0653

F/G 20/8

NL

[illegible]



MICROCOPY RESOLUTION TEST CHART
NATIONAL BUREAU OF STANDARDS-1963-A

AD-A150 964



CENTER FOR
QUANTUM ELECTRONICS AND APPLICATIONS

UNC FILE COPY

RECEIVED
MAR 11 1985
A

THE UNIVERSITY OF TEXAS AT DALLAS
BOX 688 RICHARDSON, TEXAS 75080

This document has been approved
for public release and sale; its
distribution is unlimited.

85 · 02 27 028

REPORT DOCUMENTATION PAGE		READ INSTRUCTIONS BEFORE COMPLETING FORM
1. REPORT NUMBER XXXXXX	2. GOVT ACCESSION NO. AD-A150964	3. RECIPIENT'S CATALOG NUMBER
4. TITLE (and Subtitle) Demonstration of the Feasibility of the Tuning and Stimulation of Nuclear Radiation		5. TYPE OF REPORT & PERIOD COVERED Annual Summary Report 1/1/84 - 12/31/84
7. AUTHOR(s) Carl B. Collins		6. PERFORMING ORG. REPORT NUMBER
9. PERFORMING ORGANIZATION NAME AND ADDRESS University of Texas at Dallas P.O. Box 830688 Richardson, TX 75083-0688		8. CONTRACT OR GRANT NUMBER(s) N00014-81-K-0653
11. CONTROLLING OFFICE NAME AND ADDRESS Office of Naval Research Physics Division Arlington, VA 22217		10. PROGRAM ELEMENT, PROJECT, TASK AREA & WORK UNIT NUMBERS NR 395-072 410
14. MONITORING AGENCY NAME & ADDRESS (if different from Controlling Office)		12. REPORT DATE Jan. 31, 1985
		13. NUMBER OF PAGES 34
		15. SECURITY CLASS. (of this report) Unclassified
		15a. DECLASSIFICATION/DOWNGRADING SCHEDULE
16. DISTRIBUTION STATEMENT (of this Report) Approved for public release; distribution unlimited		
17. DISTRIBUTION STATEMENT (of the abstract entered in Block 20, if different from Report)		
18. SUPPLEMENTARY NOTES <i>Cont'd</i>		
19. KEY WORDS (Continue on reverse side if necessary and identify by block number) Extreme Ultraviolet, Tunable XUV, Gamma ray laser. <i>gamma</i>		
20. ABSTRACT (Continue on reverse side if necessary and identify by block number) This project concerns the demonstration of the feasibility of the tuning and perhaps even stimulation of nuclear radiation. Theory has indicated that anti-Stokes Raman upconversion of intense but conventional long wavelength sources of radiation produced by scattering from isomeric states of nuclear excitation could lead to significant sources of tunable gamma-radiation characterized by the natural Mossbauer width of the lines. This would result in lines with sub-Angstrom wavelengths and CONTINUED OVER		

20. ABSTRACT continued

widths of a few MHz. Whether or not these processes can reach threshold depends upon the resolution of basic issues lying in an interdisciplinary region between quantum electronics and nuclear physics that have not been previously addressed. It was the purpose of this work to study these issues experimentally. Originator
Supplied keywords include:

DL14731 (Block 19)

Accession For	
NTIS GRA&I	<input checked="" type="checkbox"/>
DTIC TAB	<input type="checkbox"/>
Unannounced	<input type="checkbox"/>
Justification	<input type="checkbox"/>
By	
Date	
For	
By	
Date	
For	
By	
Date	

AI



ANNUAL SUMMARY REPORT

for the period

1 January 1984 through 31 December 1984

for

Office of Naval Research
Contract N00014-81-K-0653
Task No. NR 395-072

THE DEMONSTRATION OF THE FEASIBILITY OF THE
TUNING AND STIMULATION OF NUCLEAR RADIATION

Short Title: GAMMA RAY LASER

Principal Investigator: Carl B. Collins

The University of Texas at Dallas
Center for Quantum Electronics
P.O. Box 830688, Richardson TX 75083-0688

Reproduction in whole, or in part, is permitted for any purpose
of the United States Government.

*This document has been approved for public release and sale; its
distribution is unlimited.

PROJECT DESCRIPTION

This project concerns the demonstration of the feasibility of the tuning and stimulation of nuclear radiation. Theory has indicated that anti-Stokes Raman upconversion of intense but conventional laser radiation produced by scattering from isomeric states of nuclear excitation could lead to significant sources of tunable γ -radiation characterized by the natural Mossbauer width of the lines. Further computations have suggested that this type of coherent, as well as a type of incoherent, optical pumping could even lead to appreciable levels of inversion of the populations of nuclear levels that would be capable of supporting the growth of stimulated γ -ray intensities. Whether or not these processes can reach threshold depends upon the resolution of basic issues lying in an interdisciplinary region between quantum electronics and nuclear physics that have not been previously addressed. It is the purpose of this contract work to study these issues experimentally in order to guide the development of the technology and methods needed to exploit the enormous potential of this effect.

SCIENTIFIC PROBLEM

The viability of the concept for the tuning of γ -radiation by adding the variable energy of an optical photon produced by a tunable laser depends upon the existence in the nucleus of nearly resonant intermediate states through which the multiphoton process can proceed. Whether such states do exist is the central issue being addressed in this work. Surprisingly, such informa-

tion is currently unknown because such potentially useful states would lie in the "blind spots" of the conventional techniques of nuclear spectroscopy. Normal Mossbauer spectroscopy provides enormous resolution but a tuning range that is inadequate, by order of magnitude, to support any possible study of transitions to the intermediate states of a multiphoton process. Conversely, crystal spectrometers provide broad tuning ranges but levels of resolution that miss by two orders of magnitude the threshold that would be necessary to separate the transitions to the initial and intermediate states. As a consequence, the ideal arrangement of nuclear energy levels needed for the Raman upconversion process could be a common occurrence that has gone unnoticed because of the inadequacies of conventional nuclear spectroscopy. Thus, the critical problem has two facets: 1) the development of an appropriate spectroscopic technique and 2) the search for a suitable medium for a γ -ray laser.

A secondary issue lies also in the interdisciplinary region avoided by conventional nuclear methodology. That is the characterization of the coupling properties of the nuclear levels that would be analogous to the "kinetics" responsible for channeling an efficient portion of input energy into a single transition. Conventional methodology does not generally support the selected impulsive excitation of a single nuclear level from which fluorescence can be detected and characterized. Research is underway to demonstrate a technique for the determination of the coupling coefficients, branching ratios, and lifetimes, necessary for the evaluation of the overall dynamic efficiency for the conversion of input energy into fluorescence from selected transitions.

TECHNICAL APPROACH

For the resolution of the central issue of the existence of potentially useful intermediate states in a multiphoton upconversion of optical photons to γ -ray energies, it was first intended to demonstrate sum frequency generation in one case in which non-resonant intermediate states were known to exist. This was the case in which both initial and intermediate states were magnetic sublevels of the same nucleonic state and in which the transitions were mediated by a magnetic dipole, M1 operator. Experimental data reproduced in the literature suggested that such a process had already been, unknowingly, demonstrated for the generation of radiofrequency sidebands to Mossbauer transitions at the sum and difference frequencies. The same technique of conducting a conventional single-photon Mossbauer experiment in the presence of an intense radiofrequency field is being successfully repeated with measurement and parameterization of the conversion efficiency into the sum frequency line to determine the practical limits on the ultimate linewidths and tuning ranges that can be achieved. This technique will then be used in a bootstrap approach to support a search for accidentally resonant intermediate states. By replacing the radiofrequency excitation with tunable higher frequencies, it is expected that the tuning range of Mossbauer spectroscopy can be extended by orders-of-magnitude.

For the kinetics studies a double resonance technique is being developed that represents simply a translation into the nuclear domain of proven methods of atomic and molecular physics. A flash X-ray source will be used to pump populations of isomeric

(metastable) nuclear states to freely radiating levels. Correlation of spectrally and temporally resolved fluorescence intensities from the nuclear transitions with the pumping radiation would be used to unfold the important "kinetic" parameters, germane to efforts to optically pump a population inversion in a nuclear sample.

PROGRESS DURING THIS REPORTING PERIOD

During the past year our database was extended further to include measurements made over a larger range of incident powers and frequencies. We continued to find intense sidebands on hyperfine components of the 14.4 keV Mossbauer transition of ^{57}Fe to be maximized under conditions that minimized chances for spurious magnetostrictive effects. Prominent sidebands were observed at only tens of Watts of input power. A quantitative model was refined that explains these results in terms of coherently excited nuclear states and confirms the estimates for matrix elements critical to the overall progress toward the tuning and stimulation of nuclear radiations. Moreover, our model is able to explain 20 years of accumulated phenomenology that was supposed to have proven the magnetostrictive origin of the effect. All of the data on "geometric modification of the vibration amplitudes," transmission of phonons between media and such, are readily accommodated within the purely multiphotonic model. The places where our data contradict previous measurements are explained and the quantitative fit is quite good, as described in our recent publication in Optics Letters. The experimental details have been reported in JOSA B. Our most

recent successes have demonstrated that our procedures comprise a new technique of Nuclear Raman Spectroscopy (NRS). These are being reported in another manuscript accepted for JOSA E. Being presented there is the first NRS spectrum showing a better resolution than was obtained with conventional, single photon Mossbauer spectroscopy. Copies of these publications are found in Appendix I.

SIGNIFICANCE

The successes of the new NRS technique for nuclear spectroscopy indicate that a much higher resolution, by perhaps six orders of magnitude, can be achieved through a reasonable upgrade of the apparatus. If the range of tunability does extend to the ferromagnetic spin resonance (FSR) frequency, then it will be possible to construct a swept frequency device capable of continuously tuning over a range of 10^{11} linewidths, an enormous improvement in the state-of-the-art of nuclear spectroscopy.

APPENDIX I

REPRINTS and PREPRINTS

- Collins, C. B. and DePaola, B. D., 1985, Observation of Coherent Multiphoton Processes in Nuclear States, *Optics Lett.* 10, 25-27.
- DePaola, B. D. and Collins, C. B., 1984, Tunability of Radiation Generated at Wavelengths below 1A by Anti-Sokes Scattering from Nuclear Levels, *J. Opt. Soc. Am.* B1, 812-817.
- DePaola, B. D., S. S. Wagal and C. B. Collins, 1985, Nuclear Raman Spectroscopy, *J. Opt. Soc. Am.*, B2, (pending).

Observation of coherent multiphoton processes in nuclear states

C. B. Collins and B. D. DePaola

Center for Quantum Electronics, University of Texas at Dallas, Richardson, Texas 75080

Received July 14, 1984; accepted August 2, 1984

We have used states of nuclear excitation to demonstrate coherent multiphoton processes that were the analogs of well-known effects occurring at optical frequencies. Success in exciting radio-frequency sidebands on hyperfine components of the 14.4-keV Mössbauer transition of ^{57}Fe is described. A distinctive feature of this experiment was that the absorbing foil was rigidly bound in a graphite sandwich intended to eliminate detrimental vibrations. A model is proposed that quantitatively explains these results in terms of coherently excited nuclear states and evidentially confirms the multiphoton nature of the sidebands observed in this experiment.

We have studied the radio-frequency sidebands that can be produced on Mössbauer transitions.¹ The traditional explanations attributed this effect to periodic Doppler shifts caused by drumhead vibrations of the absorber foil that were driven by magnetostriction and fortuitously amplified by mechanical resonances.²⁻⁵ Quantitative agreement between theory and experiment was not obtained with that model.

We report here data obtained with a new experimental arrangement that was designed to eliminate drumhead vibrations and a theoretical model that appears to confirm that these radio-frequency sidebands result from the generation of large-amplitude coherent excitation of the nuclear states involved. This description accommodates all phenomena previously reported and suggests that sidebands developed in earlier experiments were driven by the same excitation of coherent states. Considerable significance can be attached to this demonstration that relatively long-wavelength radiation can serve for the efficient production of coherent nuclear excitation, which would appear to support speculations⁶ that the analogs of many of the interesting and useful processes of nonlinear optics may be found at nuclear energies.

In 1978 West and Matthias⁷ reported what seems to have been the only uncontested example of the prior excitation of a coherent nuclear state. An extremely small effect at the level of the noise was obtained in ^{181}Ta at power inputs of 1 kW. As a consequence of a more general theoretical modeling of processes of coherent nuclear excitation,⁸⁻¹¹ Olariu *et al.*⁸ reported a multiphoton model for Mössbauer transitions comparable with the Matthias model that could explain the general magnitude of the much stronger development of sidebands in the earlier ^{57}Fe experiments.

The Olariu-Matthias representation had been constructed under the assumption that the static magnetization of the absorber was fixed in direction and that only its amplitude was modulated by some tens of percent by the applied field. As a result, that model was more appropriate for nuclei embedded in paramagnetic samples. Of concern here is the more usual circumstance for ^{57}Fe in which the sample is composed of a mosaic of domains, in each of which the level of mag-

netization is uniform in direction and fixed in magnitude at the saturation value $|M_s|$. At constant temperature, $|M_s|$ is an invariant of the material, although the direction of M_s may be changed. Thus the upper, $J = 3/2$, and lower, $J = 1/2$, states of the 14.4-keV transition are split into Zeeman sublevels, each separated by $\nu_e = 25.87$ and $\nu_g = 45.49$ MHz, respectively, in pure iron.

The rather complicated response of a ferromagnetic sample to a time-varying external field has received considerable attention in studies of ferromagnetodynamics.¹² In the geometry of our work shown in Fig. 1, the sample is in the form of a thin lamina immersed only in a sinusoidally varying field, $H = H_0 \sin \omega_2 t$, lying in the plane of the foil. As was shown by Chen,¹³ in such cases, once the level of applied H has increased through the Barkhausen region and the direction of M_s coincides with the crystallographic easy direction most nearly aligned with H , intense magnetic poles are developed on the large faces by the subsequent attempts of M_s to precess around H . These poles will contribute a depolarizing field H_d to cancel the component of M_s produced by the precession normal to the surface. Precise computation of H_d is beyond the scope of this work, but Chen¹³ gives an approximation sufficient for other applications:

$$H_d = M_s \omega t \sin \phi_a \sin \omega_2 t, \quad (1)$$

where ω is the free-space spin-resonance frequency $\omega = \mu_0 \gamma |H_0|$ and ϕ_a is an angle between M_s and H in the plane. Usually $|H_d| \gg |H_0|$, and M_s subsequently undergoes a mathematically complex precession about H_d from the easy direction toward H . To facilitate this analysis, the intensity of the depolarizing field was assumed to be adequately approximated by Eq. (1) through the use of an effective average orientation angle for M_s of ϕ_a lying between the easy direction and H .

Since the natural precession frequencies for nuclei are so much lower than those for ferromagnetic spin-resonance phenomena, it is unlikely that the axes of nuclear spins can follow M_s through the nearly discontinuous Barkhausen jumps in the orientation of M_s . From a semiclassical perception, the nuclear spins should undergo a free precession having one component

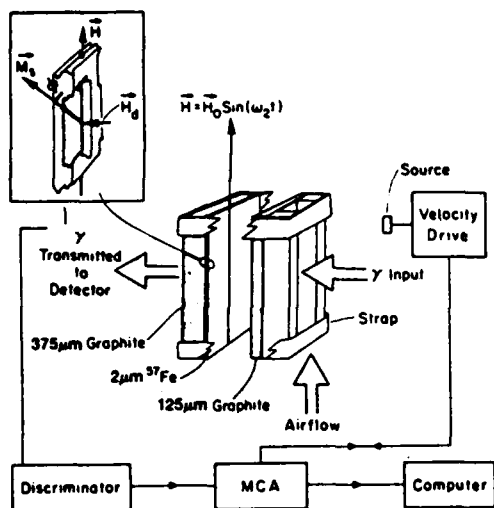


Fig. 1. Schematic representation of the experimental apparatus, together with detailed views of the foil carrier and coordinate system used in the theoretical model.

proceeding in the plane of the foil about \vec{H}_d toward \vec{M}_s , the angular velocity of which can be approximated as

$$\dot{\phi}_x = \gamma_x H_d \mu_0, \quad (2)$$

where x denotes either e for an excited nucleus or g for a ground state. This is the component that will coherently mix the nuclear states. However, another part of the precession occurs around \vec{M}_s , which results in the quantization of spin projection along \vec{M}_s . This maintains the same hyperfine splitting of the levels as exists under static conditions. Substituting Eq. (2) into Eq. (1) and integrating gives

$$\phi_x(t) - \phi_x(0) = \beta_x(\omega_g/\omega_2^2) \sin \phi_a (\sin \omega_2 t - \omega_2 t \cos \omega_2 t), \quad (3)$$

where $\phi_x(0)$ is the angle describing the orientation of spins at the end of the previous cycle of \vec{H} , $\omega_g = \mu_0 \gamma_g |\vec{M}_s| = 2\pi \times 45.49$ MHz, $\beta_g = 1$, and $\beta_e = -3|\omega_e/\omega_g|$, the negative arising because the gyromagnetic ratios are opposed in ground and excited states of ⁵⁷Fe. Limits of validity to Eq. (3) are $\omega_2 t = 0$ to π , and the expression for the return swing of the spins can be constructed from symmetry. Actual values of $\phi_x(t)$ either were taken from Eq. (3) or were set to ϕ_a or $\pi - \phi_a$ to give the smaller excursion.

At a particular time t , the effect on the quantum state of a nucleus caused by precession of the spin axis about \vec{H}_d can be determined by rotating the axis for the ground state back onto the direction defined by the spin axis of the excited state. In practice this is accomplished by multiplying the ground state with the operator for relative rotation \hat{R} , which can be expanded in a Fourier series of harmonics of the driving frequency ω_2 :

$$\begin{aligned} \hat{R} &= \exp[-i[\phi_e(t) - \phi_g(t)]\delta_d/2] \\ &= \sum_{j=-\infty}^{\infty} c_j \exp(ij\omega_2 t \delta_d/2), \end{aligned} \quad (4)$$

where δ_d is the spin matrix for rotations about the axis of \vec{H}_d and $\phi_e(t)$ and $\phi_g(t)$ are given by Eq. (3). The

result is to dress the state with $\pm j$ photons of the field, thus increasing its apparent energy relative to the excited state by $\mp j\hbar\omega_2$. The amplitude of the j th dressed state is c_j , and the relative strength of a transition between it and the reference, excited state is c_j/c_j^* . In this model that is the relative intensity of the j th sideband.

Notwithstanding the obvious difficulty that the model treats the $J = 3/2$ state as a semiclassical entity with a spin of $\pm 3/2$ and neglects mixing of its other projections, it is surprisingly good in describing the results of this experiment, even in detail. For example, a spin projection upon \vec{M}_s reverses when $\phi_e(t)$ precesses to oppose $\phi_g(t)$, so sidebands upon a forbidden transition such as $(-1/2, +3/2)$ do occur, but at energies overlapped by sidebands of $(+1/2, +3/2)$, in agreement with observation.

As can be seen from Fig. 1, the apparatus was arranged to conform completely to the traditional pattern² for this type of experiment, with one exception. This innovation lay with the foil carrier, which was arranged to sandwich the absorber rigidly between graphite sheets to prevent mechanical movements while permitting a more rapid flow of air for cooling. The conductivity was sufficient to allow significant amounts of heat to be rejected into the face of the graphite sheet during the radio-frequency pulse but not so great as to give a skin depth smaller than the physical thickness.

The radio-frequency power was applied to a coil containing the foil carrier. It was pulsed for a duration equal to the time required for the full sweep of the range of velocities being examined. The output from a proportional counter monitoring the transmitted γ intensity was gated into a multichannel scalar only during those times. Generally, duty cycles of $1/16$ prevented excessive heating of the sample. The foil used in these experiments was a 2-μm-thick, 95% pure ⁵⁷Fe sample of about 1-cm² surface area.

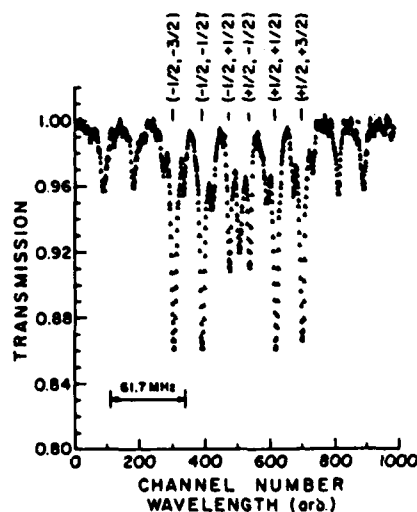


Fig. 2. Typical data obtained for pure ⁵⁷Fe at 10.1 W of radio-frequency power at 61.7 MHz. The parent transitions are identified by (M_i, M_f) , the projections of the nuclear spins in the initial and final states, respectively, upon the axis of local magnetization \vec{M}_s . The change in transition energy resulting from one additional radio-frequency photon is indicated.

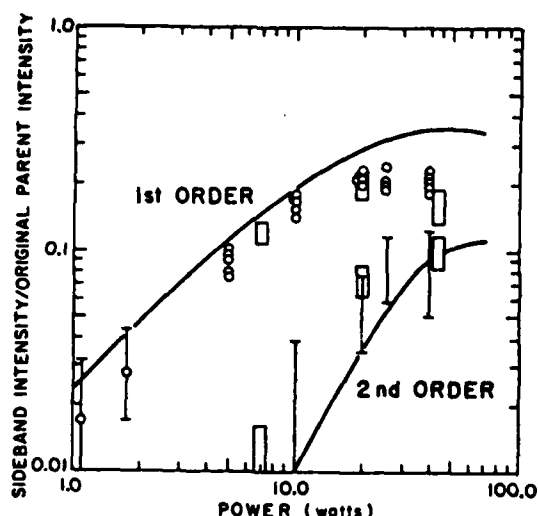


Fig. 3. Comparison of experimental and theoretical computations of sideband intensities. Differing intensities at the same power reflect the measurement of sidebands from different parent transitions. Open square symbols represent data from Ref. 3.

Figure 2 shows typical data obtained at 10 W of input power at 61.7 MHz into a resonant circuit with a $Q = 60$ that contained the coil and the foil carrier. Statistical scatter was reduced by averaging data from five successive channels. The apparent asymmetry was an artifact of the velocity drive. Any resulting uncertainty in the identity of various features was resolved by varying the frequency.

Figure 3 shows a comparison between the experimental results and the values for $c_j c_j^*$ obtained from Eq. (4). The calculated intensities depended on experimental variables through $\omega \propto |H_0| \propto \sqrt{P}$, where P is the applied radio-frequency power, and through ϕ_a , the effective orientation of M_s and H . The dependence of $c_j c_j^*$ on relative power can be seen in Fig. 3. The effect on the curves of varying ϕ_a was to change the asymptotically high levels of sideband intensity by $\pm 25\%$ of the values plotted. For the calculations of Fig. 3, $\phi_a = 0.5$ rad.

In making the comparison shown in Fig. 3 the single scale factor between the average input power and the abscissa was adjusted only once for optimal agreement, and the relative intensities were used as measured, the parent lines being assigned a value of unity in the absence of applied power. Data from Ref. 3 were normalized at the lowest power to which they fitted. Considering the rather rough, semiclassical nature of the model, the level of agreement shown in Fig. 3 is remarkable, considerably exceeding anything obtained from magnetostrictive models.³ Moreover, this model for coherent mixing of states can also explain the three classes of phenomena supposed to prove a magnetostrictive origin:

(1) Shredding or powdering the sample would provide for the development of surface poles along more than a single axis and so would inhibit or prevent free rotation of M_s .

(2) Time-varying surface poles on the face of a ferromagnetic foil could readily communicate a large, time-dependent magnetization into another material in close contact along a face.

(3) As was shown by Chen,¹³ the addition of a static field and some thickness to the sample would provide for an exponential decay of the precession of M_s after the time when excitation terminated. The phenomenon is somewhat related to spin echoes.

It seems that the strong agreement between the experimental data obtained in this work and the model of coherently excited nuclear states confirms the multiphoton nature of the transitions, whereas the observed efficiency of the effect tends to support an optimistic perspective on many of the other exciting possibilities being proposed in nuclear quantum electronics.

The authors gratefully acknowledge the support of the Office of Naval Research under contract N00014-81-K-0653.

References

1. N. D. Heiman, L. Pfeiffer, and J. C. Walker, *Phys. Rev. Lett.* **21**, 93 (1968).
2. L. Pfeiffer, N. D. Heiman, and J. C. Walker, *Phys. Rev. B* **6**, 74 (1972).
3. C. L. Chien and J. C. Walker, *Phys. Rev. B* **13**, 1876 (1976).
4. The most compelling experiments seem to have been those of Refs. 2 and 3.
5. Reviews of the extensive sideband literature are found in Refs. 7 and 8.
6. For example, multiphoton nuclear transitions and induced neutron capture and fission [S. Olariu, I. Popescu, and C. B. Collins, *Phys. Rev. C* **23**, 50 (1981)]; stimulated γ -ray emission [C. B. Collins, F. W. Lee, D. M. Shemwell, B. D. DePaola, S. Olariu, and I. I. Popescu, *J. Appl. Phys.* **53**, 4645 (1982)]; induced β -decay [N. Becker, W. H. Louisell, J. D. McCullen, and M. O. Scully, *Phys. Rev. Lett.* **47**, 1262 (1981)]; induced internal conversion, [G. C. Baldwin and S. A. Wender, *Phys. Rev. Lett.* **48**, 1461 (1982)].
7. P. J. West and E. Matthias, *Z. Phys. A* **288**, 369 (1978).
8. S. Olariu, I. Popescu, and C. B. Collins, *Phys. Rev. C* **23**, 1007 (1981).
9. C. B. Collins, S. Olariu, M. Petrascu, and I. Popescu, *Phys. Rev. Lett.* **42**, 1397 (1979).
10. C. B. Collins, S. Olariu, M. Petrascu, and I. Popescu, *Phys. Rev. C* **20**, 1942 (1979).
11. S. Olariu, I. Popescu, and C. B. Collins, *Phys. Rev. C* **23**, 50 (1981).
12. T. H. O'Dell, *Ferromagnetodynamics* (Wiley, New York, 1981), Chap. I.
13. C. W. Chen, *Magnetism and Metallurgy of Soft Magnetic Materials* (North-Holland, Amsterdam, 1977), pp. 156-170.

Tunability of radiation generated at wavelengths below 1 Å by anti-Stokes scattering from nuclear levels

B. D. DePaola and C. B. Collins

Center for Quantum Electronics, University of Texas at Dallas, Richardson, Texas 75080

Received May 1, 1984; accepted July 27, 1984

Experiments show that under certain conditions, long-wavelength radiation can be strongly coupled to the nucleus. Additional experiments demonstrate the utility of this effect as a powerful tool for nuclear spectroscopy and show how tunable subangstrom radiation can be produced. Future experiments and applications are discussed.

INTRODUCTION

There has been much written during the past 10 years about the radio-frequency (rf) sidebands that can be produced on Mössbauer transitions.¹ The traditional explanation attributed this effect to periodic Doppler shifts caused by drumhead vibrations of the absorber foil that were driven by magnetostriction and fortuitously amplified by mechanical resonances.²⁻⁴ Good quantitative agreement between theory and experiment was never achieved.

A successful multiphoton explanation was proposed by West and Matthias⁵ and independently by Olariu *et al.*⁶ In this explanation, the sidebands were described as sum- and difference-frequency lines resulting from a coherent mixing of nuclear levels by the rf fields. In contrast to the magnetostrictive model, the multiphoton model gave a good quantitative agreement with experiment. The importance of the multiphoton explanation is that it implies the existence of nuclear analogs to many of the coherent processes currently known and well understood in atomic and molecular physics. Thus many of the experimental techniques used in atomic and molecular physics may be adapted to nuclear physics. Perhaps the most immediately attractive of these is the production of tunable XUV radiation generated by anti-Stokes scattering of intense beams of more conventional form from excited nuclear levels.

In an effort to test this hypothesis, a new experiment was performed in which a ⁵⁷Fe foil was irradiated by a beam of essentially monoenergetic gamma photons and by a strong field of tunable rf radiation. The intensity of the transmitted gamma photons was then measured as a function of the rf ω_{rf} , which was varied while the gamma frequency ω_γ was held constant. This experiment may be considered the nuclear analog of Raman spectroscopy and is clearly precursive to the production of tunable XUV by the inverse process of scattering from nuclear levels.

Before this new experiment was attempted, some preliminary research was done in order to determine the appropriateness of the multiphoton theory. Therefore the first set of experiments undertaken simply repeated those of previous authors,² whereas the next set made use of a new experimental arrangement designed to reduce significantly the effect of any

accidental resonance in the foil. The results of these experiments further supported the multiphoton model and fully justified the two-photon spectroscopy experiments mentioned above.

THEORY

Although it is beyond the scope of this paper to enter into all the details of the multiphoton explanation of the rf sidebands, a general overview is, nevertheless, possible. A more detailed discussion of the theory is given in Refs. 6 and 7.

According to the nuclear multiphoton model as applied to ferromagnetic materials, an external rf field applied at a modest level of power is able to control the large internal fields seen by the nucleus. In this way, the time-varying fields are effectively amplified by many orders of magnitude to a level sufficient to dress the nuclear states. Thus the rf field is actually indirectly coupled to the nucleus through the hyperfine fields. The gamma photon then interacts with the dressed states of the system, giving rise to sidebands.

This paper is concerned with tunable, multiphoton-absorption sidebands produced on the 14.4-keV Mössbauer transitions in ⁵⁷Fe. The energy-level diagram relevant to this paper is given in Fig. 1. The 14.4-keV transition is between two different states of internal nucleonic excitation with total angular momentum values varying from $I = 1/2$ in the lower state to $I = 3/2$ in the upper. When the ⁵⁷Fe nuclei are in a ferromagnetic environment, such as is the case for a pure annealed-iron sample, the resulting net magnetic field at the nuclei removes the degeneracies; this causes both the upper and lower levels to split, giving rise to the nuclear hyperfine structure shown in the figure. In the case of Fe, the hyperfine fields are of the order of one half of a megagauss. The nucleonic transition is mediated by the magnetic-dipole operator, and so the selection rule $\Delta m = 0, \pm 1$ permits six component transitions between the lower and upper manifolds. For convenience, these are designated in the figure by the numbers 1-6, as is traditional.

The foil used in these experiments was a 2- μ m-thick, pure ⁵⁷Fe sample of about 1-cm² surface area. The usual absorption spectrum made as a function of transition wavelength in the absence of an applied rf field is shown in Fig. 2a. Typical spectra obtained in these experiments using rf fields of ~ 35

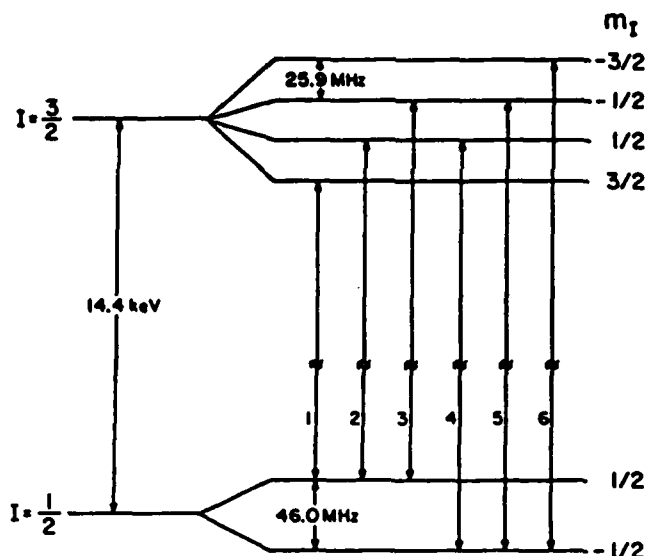


Fig. 1. Energy-level diagram for ^{57}Fe , showing the nuclear hyperfine splitting and the six magnetic-dipole-allowed transitions.

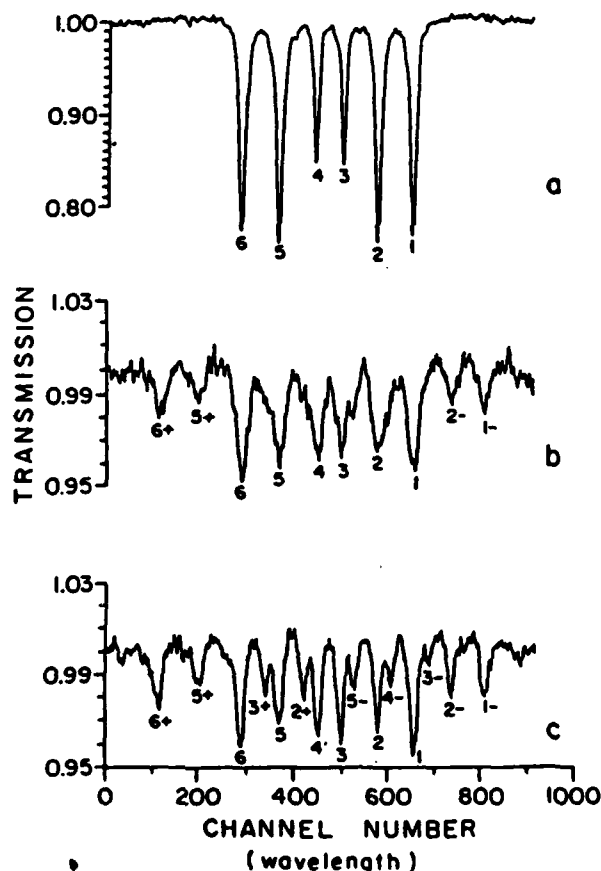


Fig. 2. a, Typical ^{57}Fe absorption spectrum with no rf applied. The six lines correspond to the six dipole-allowed transitions of Fig. 1. b, Typical spectrum using conventional sample holder with 37 W of applied rf power at 54 MHz. c, Typical spectrum using new sample holder with 31 W of applied rf power at 54 MHz.

We are shown in Figs. 2b and 2c. In these and the rest of the data presented here, the signal-to-noise (S/N) ratio was improved by a factor of $\sqrt{5}$ through the use of a running average of the data from five successively resolved wavelengths.

EXPERIMENTAL DETAILS AND RESULTS

The basic experimental arrangement is shown in Fig. 3a. The conventional Mössbauer spectrometer, an Austin Science Associates (ASA) Model S-600, could be operated in either a constant-acceleration or a constant-velocity mode. This allows the gamma-photon frequency to be Doppler shifted at a constant rate or to be held constant. The drive motor was equipped with an interferometer so that the source velocity could be monitored. The 20 μCi source was one of a typical construction for ^{57}Fe research: ^{57}Co in a Pd lattice. In this source, the active nuclei decay to $^{57}\text{Fe}^*$ by electron capture, followed by rapid decay to the upper level of the Mössbauer transition and subsequent emission of the 14.4-keV photon used in this work. Since Pd is a nonferromagnetic material, there was no net magnetic field at the source nucleus and therefore no hyperfine structure in the emission spectrum. Thus the source used in this research was an essentially monoenergetic one, having the transform-limited width contributed by the finite lifetime of the excited state.

The gamma-photon detector was a sealed proportional counter that used Kr as the fill gas and CO₂ as the quenching gas. A charge-sensitive preamplifier (ASA Model CSP 400A) amplified the signals from the proportional counter and routed them to an ASA Model LA 200 double-differentiating linear amplifier. The amplifier output was then connected to a linear gate, which provided upper and lower levels of discrimination to permit preferential selection of the pulses produced by the 14.4-keV gamma photons. The linear gate

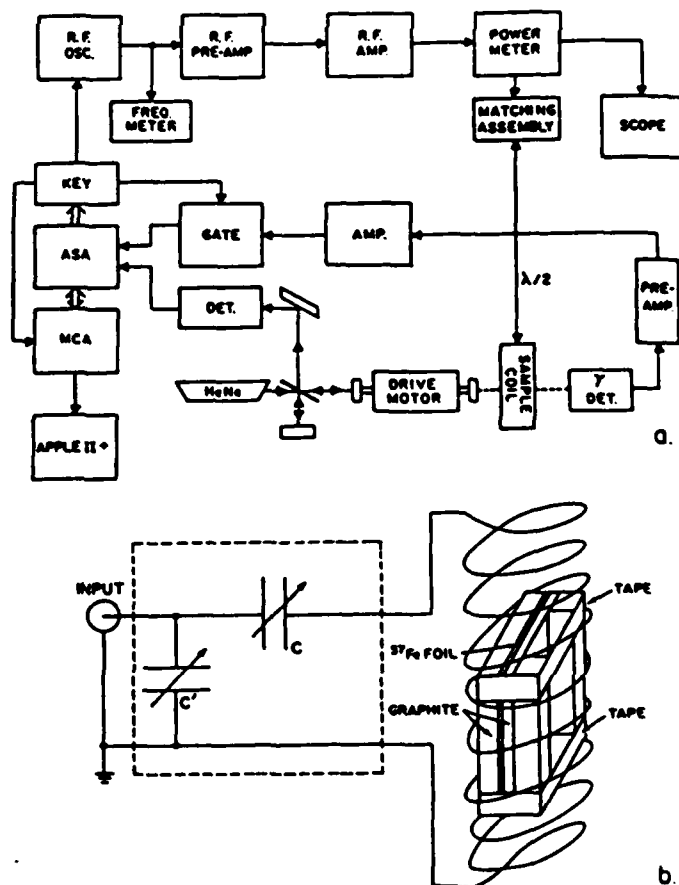


Fig. 3. a, Schematic representation of the experimental apparatus. b, Detailed view of the rf tank circuit, together with the foil carrier.

produced both a linear signal and a logic signal. The linear output was found to be useful in adjusting the gate window, and the logic signal was multiplexed with the processed interferometric signal and sent to a multichannel analyzer (MCA). The MCA was an Elscint Promeda configured for 1024-channel operation, with a rollover at 2^{17} counts per channel.

The rf apparatus consisted of an oscillator, a frequency meter, a preamplifier, an amplifier, an in-line power meter, and a parallel-series resonant LC tank circuit, as shown in Fig. 3a. The Heathkit Model IG-5280 oscillator was capable of generating a signal ranging from 0.31 to 220 MHz. It was modified to permit external keying of the rf signal. When the rf power was being applied by this keying circuit, the data from the proportional counter were gated by the ASA controller into the MCA for the time required by the drive motor to sweep through the full range of gamma frequencies to be examined. Then the keying circuit turned off the rf and closed the gate, thereby allowing enough time between pulses for the sample to cool.

The output of the oscillator was monitored by a Heathkit Model SM-2420 frequency meter and was first amplified by a Hewlett-Packard Model 8447A broadband preamplifier, which had a flat frequency response from 0.1 to 400 MHz. The signal was then sent to an ENI Model 550L amplifier, which was able to amplify rf signals over the range of frequencies from 1.5 to 400 MHz up to a power level of tens of watts. This final output passed through a Bird directional power meter, which permitted the monitoring of both forward and reflected power.

As is shown in Fig. 3b, a LC tank circuit was used to enhance the field strength actually applied to the sample. This type of circuit is of the kind commonly used in nuclear-magnetic-resonance (NMR) studies.⁸ The capacitor C together with the inductance L formed the resonant tank, and the capacitor C' served to match the impedance to the 50- Ω input cable. In this circuit, if $C' \gg C$, as was the case in our arrangement, then the resonance condition remains close to $\omega^2 LC = 1$, and the impedance at resonance is $Q\omega LC^2/(C + C')^2$, where $\omega = 2\pi\nu$ is the circular frequency of the applied rf. This impedance was matched to the 50- Ω input by tuning C' until the reflected power, as measured by the directional power meter, was at a minimum.

Estimates of the magnetic-field strength (peak to peak) inside the coil, in the absence of any ferromagnetic material, is given by $H_{rf} \approx 6(PQ/V\nu)^{1/2}$, where P is the rf power in watts supplied by the final amplifier, Q is the quality factor, V is the volume of the coil in cubic centimeters, and ν is the resonant frequency in megahertz.⁹ In the case of a coil loaded with a ferromagnetic foil, the field density is increased. This can be accommodated by replacing V by an effective volume V' . For the geometry used in our experiments, $V' \approx 1.6 \text{ cm}^3$.

The resonant frequency of the tank circuit was determined by inserting the coil of a grid dip meter (Heathkit Model HD-1250) into the coil of the tank circuit, while connecting the original input of the matching box to an oscilloscope and a frequency meter (instead of to the Bird meter's output). The grid dip meter was tuned until the signal on the scope was a maximum (typically $\sim 100 \text{ mV}$ peak to peak). The resonant frequency ν was then given by the frequency meter. After the resonant frequency was determined, the grid dip meter was adjusted both above and below it, until the signal on the scope

was at the half-power points. The Q was calculated from the frequencies at these points by the formula $Q = \nu/\Delta\nu$, where $\Delta\nu$ is defined to be the magnitude of the difference between the two half-power frequencies.¹⁰ The Q could then be used to calculate H_{rf} at the sample. For example, for the typical values of $Q = 60$, $\nu = 60 \text{ MHz}$, and $P = 25 \text{ W}$, we calculate an $H_{rf} \approx 24 \text{ O}$ peak to peak.

In our experiments, the circuit was divided into two parts in order to separate the sample physically from the rest of the electronics. The first part, the matching assembly, consisted of the two capacitors, C and C' . This entire assembly was contained in a grounded metal chassis in order to minimize stray capacitance as well as radiation of the rf signal. The two capacitors were tuned by turning micrometer shafts that penetrated the box through two small holes. The second part of the resonant circuit consisted of the coil in which the ^{57}Fe foil was placed. The coil was a simple helix of eight turns, wrapped about a polyvinyl chloride (PVC) tube for extra stability. The tube had windows cut in it so that signal attenuation and line broadening resulting from the nonresonant absorption of the gamma photons by the PVC was minimized. Like the matching assembly, the coil and the sample were contained in a grounded metal chassis. Although the end of the PVC tube protruded from the box in order to provide a cooling chimney, stray radiation from this hole was judged to be minimal because it lay on the axis of the coil.

The Fe sample was mounted in a special holder that fitted into the coil, and herein lay the principal innovation: Whereas the samples in previous experiments had been typically held between Mylar or Lucite sheets, ours was rigidly clamped between two graphite sheets that were thin enough to allow penetration of the rf field but thick enough to prevent any drumhead vibrations of the foil. Graphite seems to be an ideal substance for this purpose. Having a skin depth of $205 \text{ }\mu\text{m}$ at 60 MHz , it is, nevertheless, a reasonably good conductor of heat, and it is almost transparent to the 14.4-keV photons used in these experiments. The graphite sheet on the source side of the foil was $\sim 125 \text{ }\mu\text{m}$ thick, and the sheet on the detector side was $\sim 375 \text{ }\mu\text{m}$. The second sheet was a little thicker to provide extra rigidity for the sample. This arrangement also allowed the possibility of cooling the foil by immersing it in liquid N_2 without the random motion caused by boiling the liquid. An additional advantage was that the effect of joule heating in the foil was minimized because the heat was extracted along the entire surface in contact with the graphite. The discriminator window did need to be adjusted slightly to maximize the 14.4-keV output with the graphite installed.

The two parts of the resonant tank circuit were linked together by a coaxial cable. Because this cable was one-half wavelength long, it is designated in Fig. 3 by $\lambda/2$. The speed of signal propagation in coaxial cable is about $1.8 \times 10^8 \text{ m/sec}$.⁸ Therefore, for a frequency of 60 MHz , a cable of length $1.8 \times 10^8 / (2 \times 60 \times 10^6)$ or 1.5 m was used. The purpose of the half-wave line was to isolate the inductor physically from the tuning and matching capacitors, allowing the sample, coil and all, to be immersed in liquid N_2 , if necessary, without condensation building up on any of the other circuit components. For the new results presented here, the power required to produce sizable sidebands was so low that no cooling schemes (other than forced convection through the PVC chimney by a small blower) were necessary. The half-wave line did have

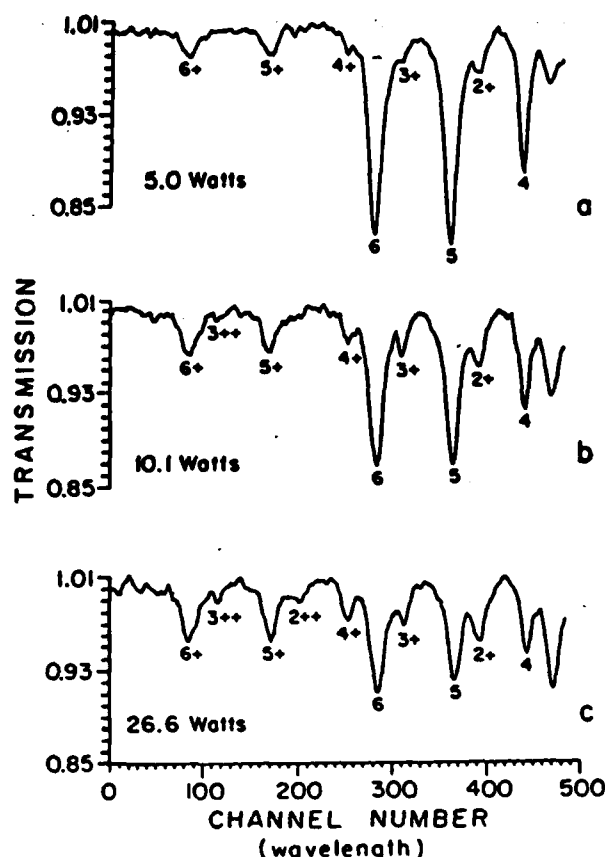


Fig. 4. Three 61.7-MHz spectra, showing the power dependence of the first-order sidebands. a, 5.0-W rf power. b, 10.1-W rf power. c, 26.6-W rf power.

the disadvantage that it was not a broad-bandwidth device, and so there was only about 10% tunability before the installation of a new line was necessary. However, because of the narrow range of frequencies being investigated, only a few different cables were needed.

The first sequence of experiments simply repeated those already reported by other authors, in which the foil had free surfaces. The foil was cooled by immersing it in a gentle stream of cool N_2 vapor. For a given run, the radio power and frequency were held constant, while the gamma frequency was continuously Doppler shifted by using the spectrometer driver motor in flyback (constant-acceleration) mode. Figure 2b shows part of a typical spectrum for this sequence of experiments. We use the convention whereby sidebands are labeled by the parent line from which they come, and by one or more pluses or minuses, indicating positive (high-energy) or negative (low-energy) sidebands, respectively, from states dressed by the number of rf photons corresponding to the number of pluses or minuses. In Fig. 2b, the applied rf power was 37 W, and the frequency was 54.1 MHz. Note that, whereas the sidebands clearly exist, the S/N ratio is not good. The marked asymmetry in the spectrum was caused by a corresponding asymmetry in the drive motors. Any resulting uncertainty in the identity of various features was resolved by varying the frequency.

The next round of experiments differed from the previous round only in that the new sample holder was used to suppress drumhead vibrations and no cooling scheme other than forced

convection was used. A typical spectrum is shown in Fig. 2c. For this spectrum, the radio power and frequency were 31 W and 54.1 MHz, respectively. Note that, because of a greatly improved S/N ratio (presumably the result of better cooling and fewer random vibrations of the sample foil), the spectrum is much cleaner, and the sidebands themselves are narrower and much greater in magnitude. Also, note how, because of the increased resolution, first-order lines in the interior of the spectrum, whose presence is only hinted in Fig. 3b, stand out sharply. Prevention of any drumhead vibrations of the foil markedly improves the quality and magnitude of the sidebands; this is interpreted as evidence against the magnetostriction model. This interpretation seems justified since proponents of that model have claimed that when nonmetallic materials, such as grease, adhesive tape, and Plexiglas, were put in close contact with the foil, the sidebands were quenched owing to the damping of acoustic vibrations.¹¹ However, we believe that the observed quenching was solely due to the trapping of heat in the sample and the consequent degradation of the spectra.

Figure 4 shows how the first-order sidebands grow as a function of applied rf power. For spectra a, b, and c, $\omega_{rf} = 2\pi \times 61.7$ MHz, and the power was 5.0, 10.1, and 26.6 W, respectively. For all these spectra, as well as for the rest of the data presented here, the improved sample holder was used. The first-order sidebands are seen to grow linearly with applied rf power until finally saturating. In Fig. 4c, at a power of only 26.6 W, the second-order sidebands are already beginning to become apparent. On application of even higher

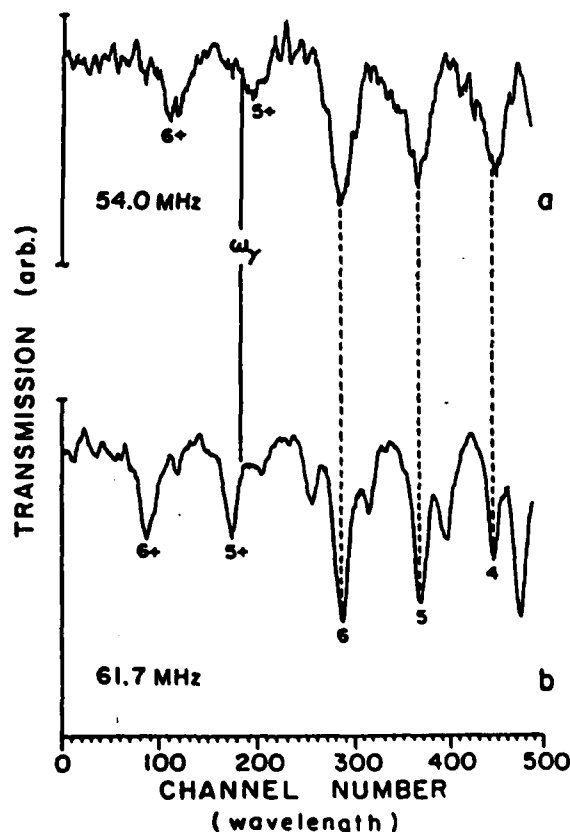


Fig. 5. Two spectra that show that the result of increasing ω_{rf} is to push first-order sidebands away from the parents, through a two-photon resonance at ω_{γ} .

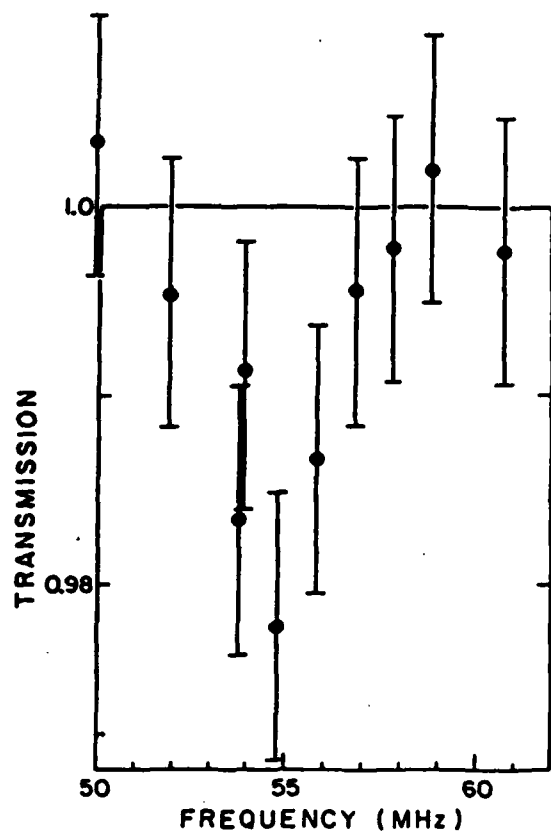


Fig. 6. Absorption resonance corresponding to the first-order sum-frequency sideband of the $|1/2, 1/2\rangle \rightarrow |3/2, 1/2\rangle$ nuclear transition of ^{57}Fe near 0.086 nm.

rf-field intensities, the second-order sidebands were seen to grow quadratically and finally to saturate. These results are exactly the kind predicted by the multiphoton theory, which lends further support to that explanation. According to this theory, the saturation of the first-order lines occurs because the second-order lines, which grow as the square of applied power, begin to gain importance; and the second-order lines are predicted to saturate when higher-order sidebands begin to grow. For a more complete discussion of the theory as applied to ferromagnetic materials, see Ref. 7.

In the final set of experiments described here, the gamma-photon frequency was held fixed by using the spectrometer motor in constant-velocity mode, the rf-field strength was held constant, and ω_{rf} was varied. Figure 5 helps to explain the experiment. Figure 5a is part of a normal sideband spectrum with $\omega_{rf} = 2\pi \times 54$ MHz, whereas in 5b, $\omega_{rf} = 2\pi \times 61.7$ MHz. With a constant source velocity of 7.78 mm/sec, the frequency of its gamma photons, ω_γ , would lie at the position indicated, regardless of ω_{rf} . The effect of increasing ω_{rf} is to push the sidebands away from the parents, through the two-photon resonance at ω_γ . As ω_{rf} is varied, point by point, the gamma intensity is monitored. Because the tank circuit had to be retuned, and the Q had to be measured for each frequency, only one data point was taken per run.

In Fig. 5 the movement of the 5^+ sideband is shown for clarity. In the actual experiment, the source velocity was set to 3.2 mm/sec, allowing the 2^+ sideband to be examined in a spectrally isolated region. The resulting spectrum is shown

in Fig. 6. The error bars are quite large because of the short accumulation time allowed for each frequency.

DISCUSSION

Although the quality of the spectrum in Fig. 6 is no better than that of Fig. 2b in terms of S/N ratio, the result is, nevertheless, quite important. The fact that a two-photon nuclear resonance can be detected by varying the longer-wavelength photon has significant implications. For example, if the quality of the spectrum were improved through longer accumulation times, the technique could be used to conduct Mössbauer spectroscopy with much higher resolution than ever before. This would be possible because *no mechanical tuning need be used*. In addition, if the technique were extended from rf to microwave or infrared photons, the range of Mössbauer spectroscopy would be dramatically increased. With this kind of tool, a great deal of new information can be gained about the nucleus, since conventional nuclear spectroscopy is limited in either resolution (~ 100 eV for the gamma-fluorescence type of experiments) or range of tuning ($\sim 10^{-4}$ eV for Mössbauer studies).

Although in our experiments the strong hyperfine fields in a ferromagnetic sample were utilized in order to couple the rf photons to the nucleus, the two-photon technique is, in fact, far more general. For example, ferroelectrics, which have a strong electric-field gradient (EFG), could also be used. Here, instead of modulating a strong magnetic field, the rf field would dress the nuclear states by modulating the EFG at the site of the nucleus. Since it is often possible to place a given nuclear species at a desired crystal-lattice position (by diffusion or some form of ionic substitution), the two-photon technique could be used on an extremely large number of different nuclear species.

Another exciting possibility is the generation of tunable subangstrom radiation. In the context of our experiments, if the ^{57}Co had been in a ferromagnetic environment and had been subjected to the rf fields, then the result would have been an emission spectrum with tunable sidebands. The parent lines could then have been filtered out with a thin sheet of ^{57}Fe , leaving just the tunable, narrow-linewidth, subangstrom radiation. These and several other exciting possibilities are discussed in Ref. 12.

CONCLUSIONS

In this paper, the results of three different sets of experiments were reported. The first set repeated the conventional rf sideband experiments. In the second set of experiments, a novel sample holder was used, which restricted the movements of the foil. In the resulting spectra, the sidebands were of greater magnitude and better quality, implying that, contrary to the magnetostriction model, fortuitous vibrations and mechanical resonances in the foil did not contribute to the generation of the sidebands.

In the final series of experiments, the multiphoton nature of the sidebands was exploited to generate a spectrum of gamma-photon transmission intensity as a function of ω_{rf} . These experiments constituted a nuclear analog to Raman spectroscopy.

It was suggested that with certain modifications, these experiments would produce subangstrom, narrow-bandwidth radiation, tunable over several linewidths.

Finally, other experiments were proposed in which, through exploitation of the strong EFG in ferroelectric materials, one could use anti-Stokes scattering in the nucleus to investigate the properties of whole classes of nuclear species.

ACKNOWLEDGMENT

The authors gratefully acknowledged the support of the Office of Naval Research under contract N00014-81-K-0653.

REFERENCES

1. Reviews of the extensive sideband literature are found in Refs. 5 and 6.
2. N. D. Heiman, L. Pfeiffer, and J. C. Walker, "Rf-induced sidebands in Mössbauer spectra," *Phys. Rev. Lett.* **21**, 93-96 (1968).
3. L. Pfeiffer, N. D. Heiman, and J. C. Walker, "Mössbauer sidebands by rf excitation of magnetic materials," *Phys. Rev. B* **6**, 74-89 (1968).
4. C. L. Chien and J. C. Walker, "Mössbauer sidebands from a single parent line," *Phys. Rev. B* **13**, 1876-1879 (1976).
5. P. J. West and E. Matthias, "Frequency modulation of the 6.2 keV Mössbauer states of ^{181}Ta ," *Z. Phys. A* **288**, 369-372 (1978).
6. S. Olariu, I. Popescu, and C. B. Collins, "Multiphoton generation of optical sidebands to nuclear transitions," *Phys. Rev. C* **23**, 1007-1014 (1981).
7. C. B. Collins and B. D. DePaola, "Tunable sub-angstrom radiation generated by anti-Stokes scattering from nuclear levels," *AIP Conf. Proc.* (to be published).
8. E. F. Fukushima and S. B. Roeder, *Experimental Pulse NMR, a Nuts and Bolts Approach* (Addison-Wesley, Inc., Reading, Mass., 1981), Chap. 3.
9. W. G. Clark, "Pulsed nuclear resonance apparatus," *Rev. Sci. Instrum.* **35**, 316-333 (1964).
10. R. E. Simpson, *Introductory Electronics for Scientists and Engineers* (Allyn and Bacon, Boston, Mass., 1974), Chap. 2.
11. M. Kopcewicz and A. Kotlicki, "Mössbauer study of the separation of the rf sideband and collapse effects in Invar," *J. Phys. Chem.* **41**, 631-633 (1980).
12. C. B. Collins, F. W. Lee, D. M. Shemwell, and B. D. DePaola, "The coherent and incoherent pumping of a gamma ray laser with intense optical radiation," *J. Appl. Phys.* **53**, 4645-4651 (1982).

Nuclear Raman Spectroscopy

by

B. D. DePaola, S. S. Wagal, and C. B. Collins

Center for Quantum Electronics

University of Texas at Dallas

Richardson, TX 75080

ABSTRACT

An experiment is described in which the nuclear analog to Raman spectroscopy has been applied to ^{57}Fe . The results of the experiment are given, and future applications of the technique are proposed.

This communication reports major progress toward our overall goals of demonstrating the feasibility of tuning, and ultimately of stimulating, the emission of gamma radiation. Theory [1-5] developed over the past five years has shown the inherent viability of many of the analogs for nuclear excitation of the familiar concepts of quantum electronics. Model studies [5,6] have shown that hardware requirements to achieve threshold for stimulated emission in the sub-Angstrom region would resemble lasers currently used in inertial fusion studies, but that threshold should be accessed at substantially lower pump energies than will be needed for breakeven. It appears that existing devices might prove adequate *if suitable isotopes actually exist*. This is the critical point. Despite the many applications of beautiful and involved techniques of nuclear spectroscopy, the current data base is inadequate in both coverage and resolution either to answer the question of whether an acceptable isotope exists, or to guide in the selection of a possible candidate medium for a gamma ray laser.

To experimentally evaluate the feasibility of tuning and stimulating gamma radiation has required an iterative approach. As recently reported, [7] the absolute scale of the matrix elements important to the realization of the nuclear analogs to the various possible frequency mixing processes was confirmed to agree with theory. Incidentally,

this implied that the techniques of nuclear spectroscopy could be extended in the direction needed to support a search for gamma ray laser media by exploiting a type of multiphoton Mössbauer spectroscopy suggested by the same theories. Subsequently, the experimental feasibility of such a technique was reported [8]. Described here are the most recent results confirming the practicality of the resulting methodology denoted Nuclear Raman Spectroscopy in this work.

Nuclear Raman Spectroscopy (NRS) is a type of Mössbauer absorption spectroscopy, in which the intensity of transmitted, single-frequency gamma photons is measured as a function of the frequency of a second, long wavelength, photon field in which the nuclei are immersed. There are several advantages of NRS over more conventional Mössbauer techniques. One of these is the potential for an increased frequency resolution in the spectrum. This would be possible because the frequency of the long wavelength photons can be controlled to a much higher degree than that of the gamma photons.

Another advantage of NRS is the potential for extending the range of nuclear spectroscopy. Using current techniques, one is typically limited either in resolution (~ 100 eV for gamma fluorescence type experiments), or range ($\sim 10^{-4}$ eV for conventional Mössbauer studies). If the NRS technique were extended to use coherent microwave or

infrared sources of variable frequency photons, a great deal of new information could be learned about the nucleus.

As mentioned above, in a previous article [8] some early efforts in NRS were reported. In those experiments, the feasibility of that technique was experimentally demonstrated, using an rf field as the source of long wavelength photons. A problem associated with those experiments was a relatively low Signal to Noise ratio (S/N), resulting both from short data accumulation times and slight fluctuations in rf power levels for different frequencies. Those difficulties have been overcome in this work.

The energy level diagram relevant to the absorber foil used in this work is given in Figure 1. The splitting in the upper and lower manifolds is caused by the presence of strong static magnetic fields in the material. The selection rule $\Delta m = 0, \pm 1$ allows six component transitions between the lower and upper manifolds. For convenience, these are designated in the figure by the numbers 1-6, as has been traditional in nuclear physics. Sidebands to these single photon transitions (often referred to as parent lines) are given the same number labeling their parents, followed by one or more plus or minus signs, indicating positive (high energy) or negative (low energy) sidebands respectively, from states dressed by the number of rf photons corresponding to the number of plus or minus signs.

Figure 2 represents the results of a series of experiments [7], designed to determine the dependance of sideband intensity on applied power. The measured sideband intensities were first normalized by dividing them by the intensity of their parents. The upper curve gives the dependance of the first order sideband intensity on rf power, while the lower curve gives the dependance of the second order sideband intensity on rf power. As will be shown, these curves proved useful in the analysis of the NRS data.

The new experiment was carried out in the following way: An ^{57}Fe foil was irradiated by a beam of essentially mono-energetic gamma photons, and by a strong field of tunable radio frequency radiation. The intensity of transmitted gamma photons was then measured as a function of the radio frequency ω_{rf} which was varied, while the gamma frequency ω_γ was held constant. The gamma photon frequency was held fixed by using a conventional Mössbauer spectrometer motor in constant velocity mode. The rf field strength in the sample foil was held as constant as possible, and ω_{rf} was varied at the oscillator. Because an LC tank circuit, which was used to enhance the rf field, had to be re-tuned, and its Q had to be measured for each frequency, only one data point, the average of 1024 channels in a multichannel analyser, was taken per run. Further details of the experimental arrangement are given in

reference [8].

Figure 3 helps to further explain the experiment. Figure 3a is part of a conventional Mössbauer spectrum in which the tuning resulted from progressively increasing Doppler shifts produced mechanically. Clearly displayed in Figure 3a is a typical sideband spectrum with $\omega_{rf} = 2\pi \times 54$ MHz, while in 3b, $\omega_{rf} = 2\pi \times 61.7$ MHz. With a constant source velocity of 7.78 mm/sec, the frequency of the gamma photons, ω_γ would lie at the position indicated, regardless of ω_{rf} . The effect of increasing ω_{rf} is to "push" the sidebands away from the parents, through the two photon resonance at ω_γ .

Each data point was corrected for input power fluctuations and the Q of the LC tank for each frequency, as well as for the weakening of the gamma source with time, by the formula:

$$S'_n = \frac{\left[B - S_n \exp\left(-\frac{t}{\tau}\right) \right] f(P_s)}{f\left(\frac{P_n Q_n}{Q_s}\right)}, \quad (1)$$

where S_n is the n^{th} unprocessed data point, P_n is the power read with a directional power meter, Q_n is the quality factor of the LC tank circuit for the n^{th} data point, t is the relative age of the source (in days), and B is the

baseline of the spectrum. The symbol τ in this expression is equal to the half-life of ^{57}Co (~ 271 days), divided by the natural logarithm of 2. The function $f(P_n)$ is given by the upper curve in Figure 2, and was useful in normalizing all the data to a "standard" power and Q factor (i.e. for $n = s$) of 12.2 Watts and 50.8, respectively. The resulting spectrum is shown in Figure 4. The triangles represent the normalized data points, while the solid curve in the figure is the best fit of these points to the sum of two Lorentzians subtracted from a constant baseline. The Simplex algorithm [9] was used to fit this function to the data.

Theoretically, the function to be fit to the data should be of the following form:

$$S = B - (L_1 + L_2) \quad , \quad (2)$$

where

$$L_n = \frac{h_n \sigma_n^2}{\sigma_n^2 + (\omega_{0n} - \omega_{rf})^2} \quad , \quad (3)$$

Here, h_n is the maximum "height", σ_n is the Half Width at Half the Maximum (HWHM), and ω_{0n} is the center of the n^{th} Lorentzian; and B is the baseline. This means that for the two absorption lines in Figure 4, seven parameters had to be fit to the data.

The estimated standard deviation of the resulting

curve is $< 5\%$. The minima in the solid curve are within ~ 1 MHz of their theoretical positions. This is not unreasonable agreement considering there are only 14 data points spread over a range of 15 MHz.

In addition to the expected, $5+$ first order sideband to transition #5, appearing at 59.7 MHz, an additional absorption line appears at 54.1 MHz. This corresponds to $3++$, the second order sideband to transition #3. The separation between these two lines is also within ~ 1 MHz of the theoretical value.

There were several potential sources of error in this experiment and they will now be discussed. First of all, with only 14 data points to span a 15 MHz interval, better resolution along the frequency axis could not be expected. Obviously, the small number of points precluded the use of a running average in order to reduce the statistical fluctuations in the signal. In addition, because there were only twice as many data points as there were parameters to fit, the "best fit" of the data to the expected function must be viewed with caution.

A final source of error resulted from the method used to normalize the data. As mentioned in the explanation of Equation (1), $f(P_n)$ is given by a plot of observed first order sideband intensity as a function of applied power, (measured at the directional power meter). In fact, this procedure is not valid for points which are affected by a

second or higher order sideband. Unfortunately, there was no satisfactory way to deal with this problem: The spectra could not be deconvolved until the points were first normalized, and the points could not be properly normalized until the spectra was sufficiently deconvolved to weight the normalization process. In the case of the data shown in Figure 4, the input powers and Q_s were close enough in value that the correction factors were all < 2 , (with most < 1.3).

One way that this last error could have been eliminated is by tuning the gamma photon frequency to be less than that required to make transition #1, by an amount greater than the sum of the total widths of the two manifolds. Then, by applying an rf field with a high enough frequency, that is for ω_{rf} ranging from $2\pi \times 124$ to $2\pi \times 202$ MHz, the entire upper manifold could be seen as first order sidebands with no second order lines entering the spectrum. Unfortunately, because of the limitations of the LC tank circuit used in this work, the highest frequency that could be used was well below this amount.

In any case, the point of the experiment was not to characterize the energy levels of ^{57}Fe , but to demonstrate the effectiveness of a new technique for nuclear spectroscopy in general, based on multiphoton effects. In practice, the method would probably be most useful with the rf field being replaced by a microwave or infra-red photon field. The fact that a two photon nuclear resonance can be

detected by varying the longer wavelength photon has significant implications. For example the technique could be used to conduct Mössbauer spectroscopy with much higher resolution than ever before. This would be possible because no mechanical tuning need be used. In addition, if the technique were extended from rf to microwave or infrared photons, the range of Mössbauer spectroscopy would be dramatically increased.

The authors gratefully acknowledge the support of the Office of Naval Research under Contract N00014-81-K-0653.

References

- [1] C. B. Collins, S. Olariu, M. Petrascu, and I. Popescu, "Enhancement of γ -Ray Absorption in the Radiation Field of a High-Power Laser," *Phys. Rev. Lett.* **42**, 1397-1400 (1979).
- [2] C. B. Collins, S. Olariu, M. Petrascu, and I. Popescu, "Laser-Induced Resonant Absorption of γ Radiation," *Phys. Rev. C* **20**, 1942-1945 (1979).
- [3] S. Olariu, I. Popescu, and C. B. Collins, "Tuning of γ -Ray Processes with High Power Optical Radiation," *Phys. Rev. C* **23**, 50-63 (1981).
- [4] S. Olariu, I. Popescu, and C. B. Collins, "Multiphoton Generation of Optical Sidebands to Nuclear Transitions," *Phys. Rev. C* **23**, 1007-1014 (1981).
- [5] C. B. Collins, F. W. Lee, D. M. Shenwell, and B. D. DePaola, "The Coherent and Incoherent Pumping of a Gamma Ray Laser with Intense Optical Radiation," *J. Appl. Phys.* **53**, 4645-4651 (1982).
- [6] C. B. Collins in AIP Conference Proceedings No. 90, Laser Techniques for Extreme Ultraviolet Spectroscopy, ed. T. J. McIlrath and R. R. Freeman, pgs. 454-464 (AIP, 1982).
- [7] C. B. Collins and B. D. DePaola, "Observation of Coherent Multiphoton Processes in Nuclear States," (to be published).

- [8] B. D. DePaola and C. B. Collins, "Tunability of Radiation Generated at Wavelengths below 1A by Anti-Stokes Scattering from Nuclear Levels," (to be published).
- [9] M. S. Caceci, and W. P. Cacheris, "Fitting Curves to Data," Byte, May 340-362 (1984).

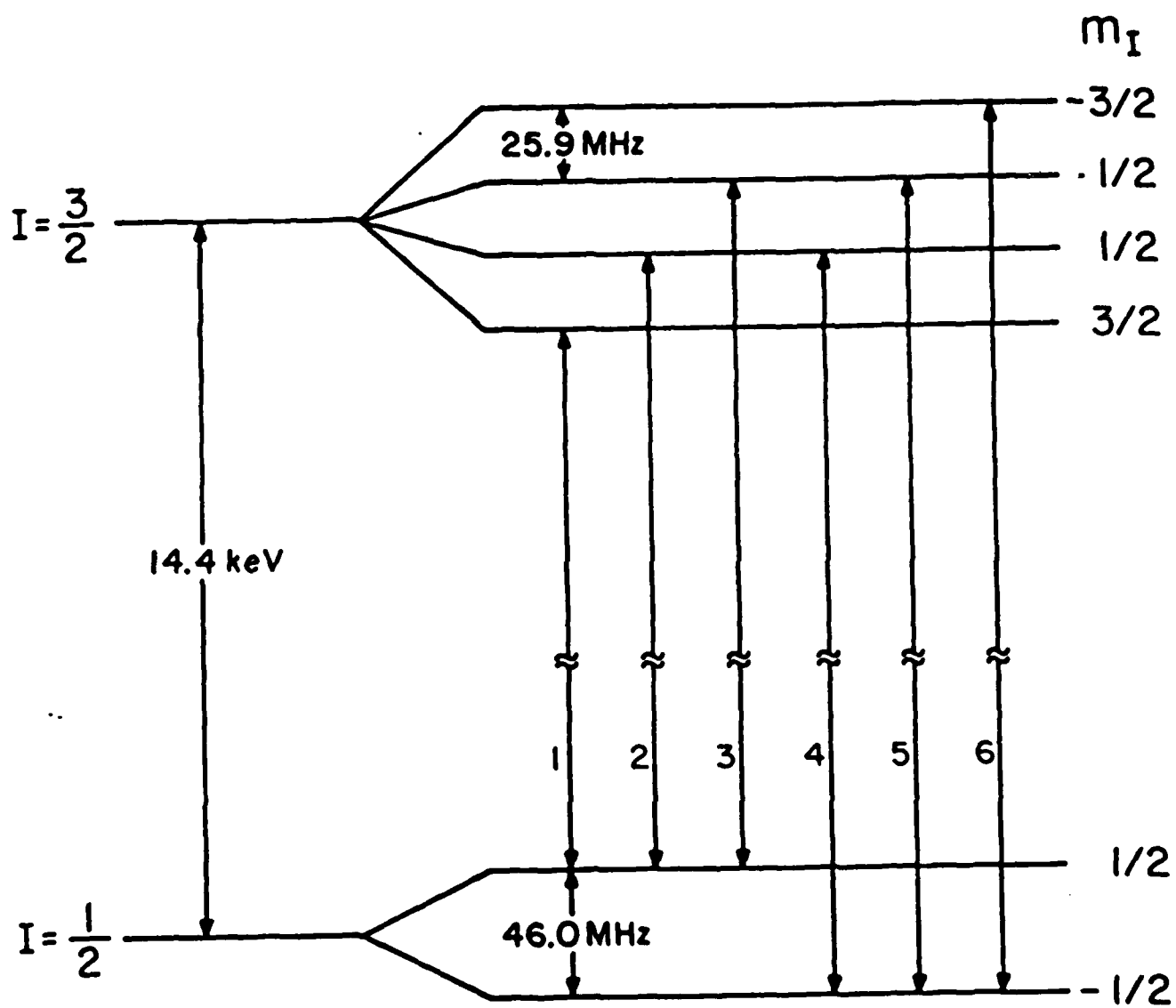
CAPTIONS

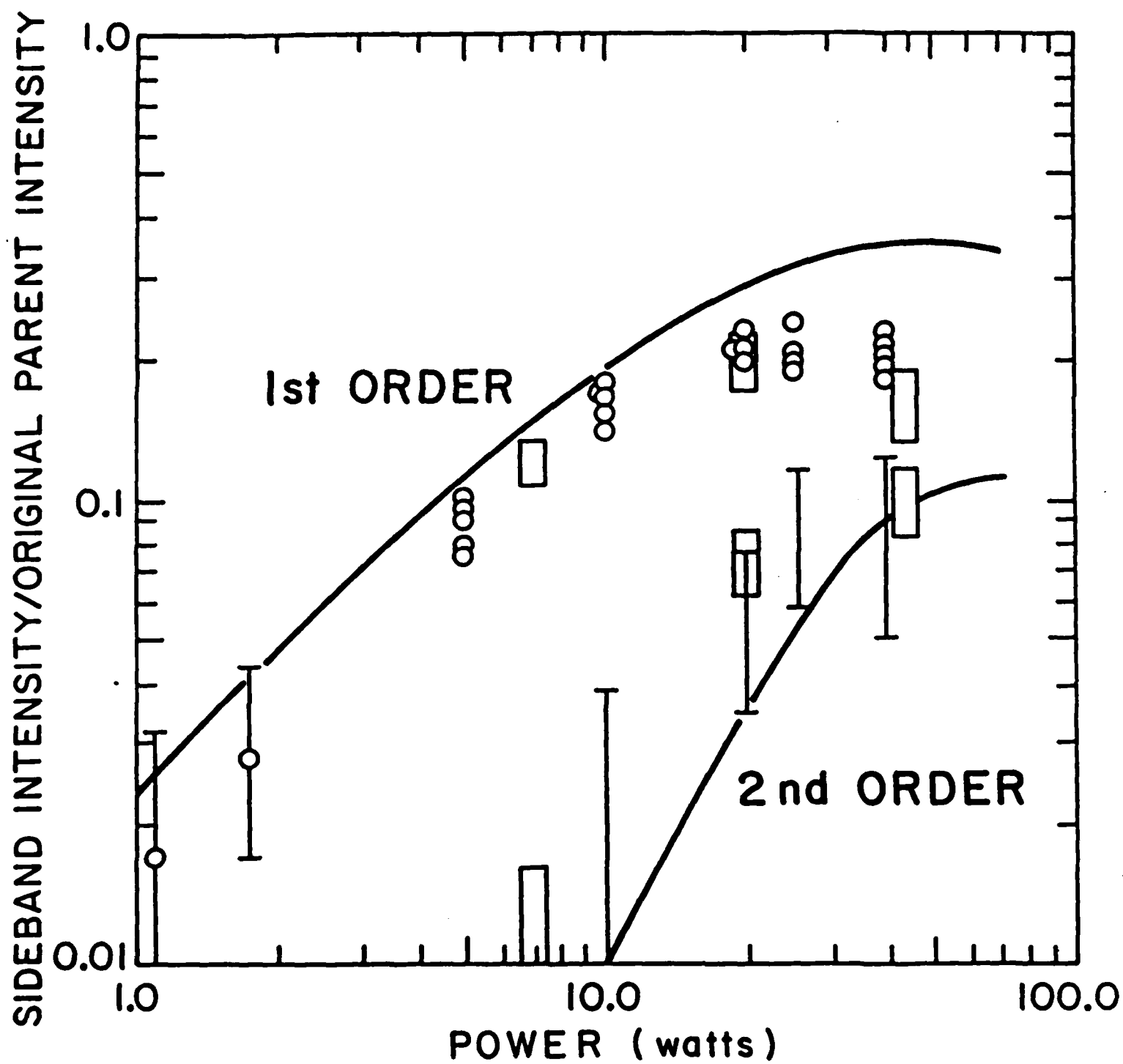
Figure 1: Energy level diagram for ^{57}Fe , showing the nuclear hyperfine splitting, and the the six magnetic dipole-allowed transitions.

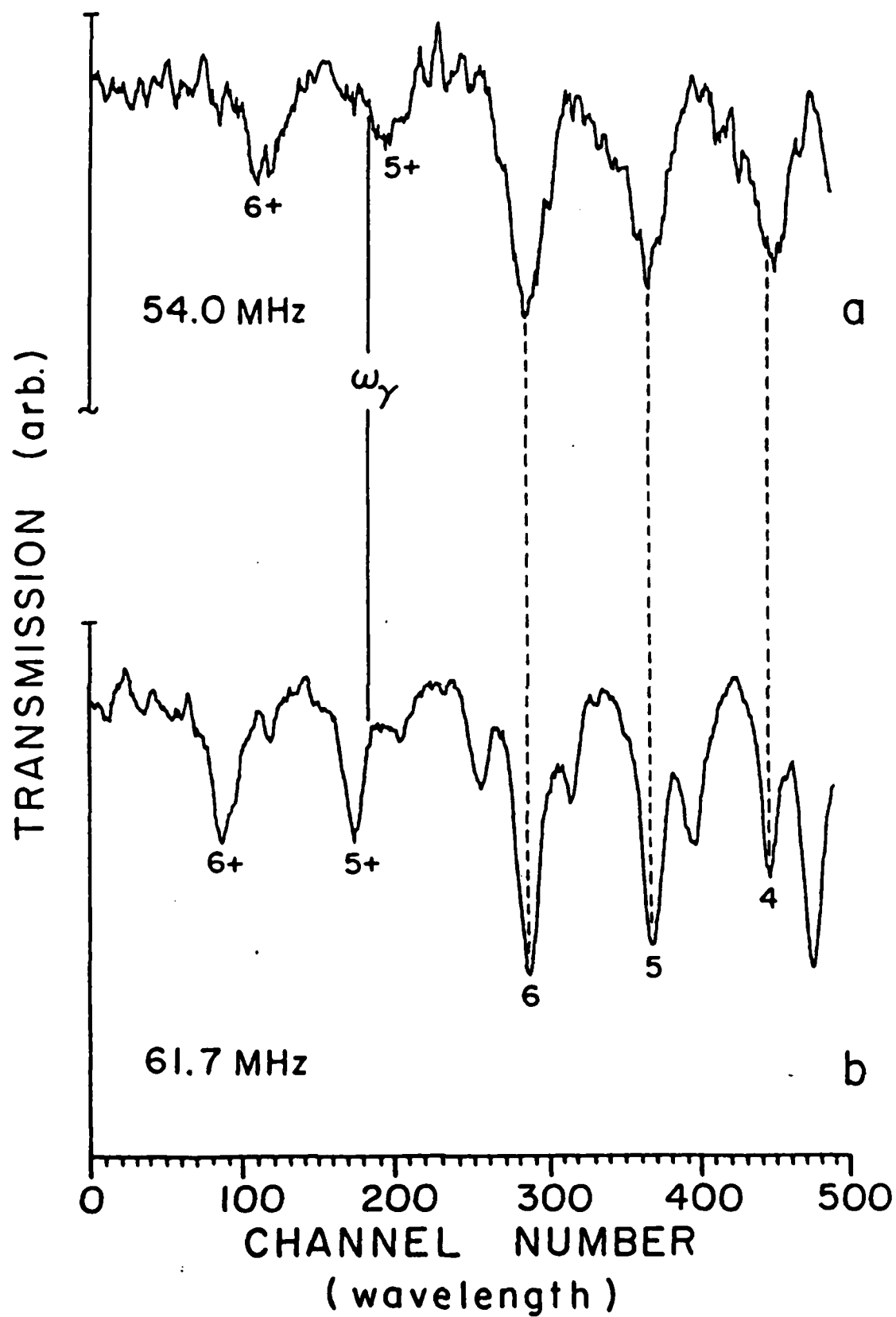
Figure 2: Comparison of experimental and theoretical computations of sideband intensities. Differing intensities at the same power reflect the measurement of sidebands from different parent transitions. (See reference x for a more detailed explanation.)

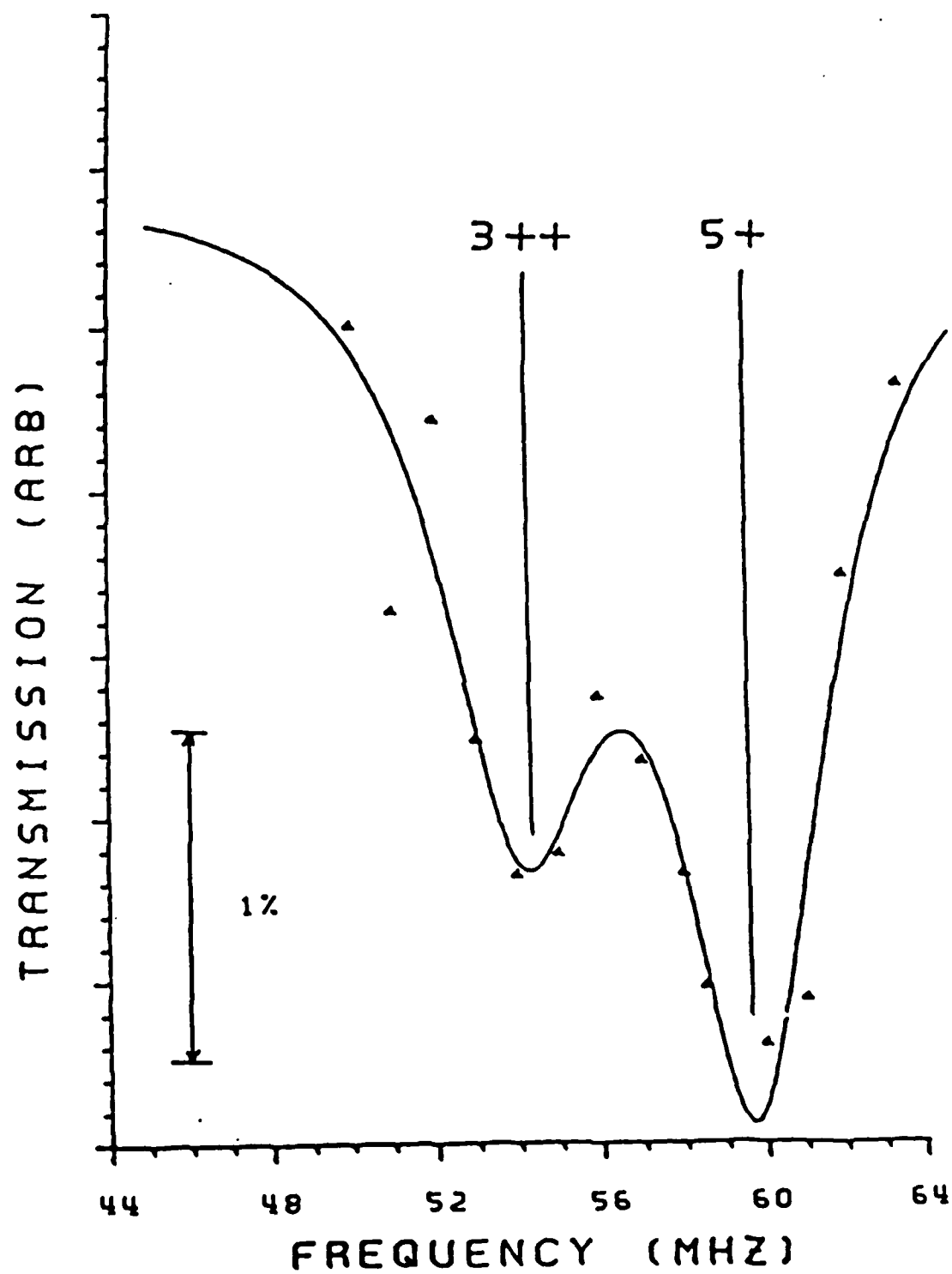
Figure 3: Two spectra which show that the result of increasing ω_{rf} is to push first order sidebands away from the parents, through a two photon resonance at ω_{γ} .

Figure 4: Gamma transmission intensity plotted as a function of rf photon frequency. The larger absorption line corresponds to the first order, sum frequency sideband of the $|1/2, -1/2\rangle \rightarrow |3/2, -1/2\rangle$ nuclear transition of ^{57}Fe , while the smaller line corresponds to the second order, sum frequency sideband of the $|1/2, 1/2\rangle \rightarrow |3/2, -1/2\rangle$ transition.









END

FILMED

4-85

DTIC